INTERNATIONAL JOURNAL OF NUMERICAL METHODS IN FLUIDS, VOL. 13, 625–641 (1991)

COMPUTER-AIDED SPILLWAY DESIGN USING THE BOUNDARY ELEMENT METHOD AND NON-LINEAR PROGRAMMING

H. C. HENDERSON

Faculty of Technical Mathematics and Informatics, Delft University of Technology, Julianalaan 132, NL-2500 AE Delft, The Netherlands

M. KOK

Rivers, Navigation and Structures Division, Delft Hydraulics, PO Box 152, NL-8300 AD Emmeloord, The Netherlands

AND

W. L. DE KONING

Faculty of Technical Mathematics and Informatics, Delft University of Technology, Julianalaan 132, NL-2500 AE Delft, The Netherlands

SUMMARY

The general context of this paper is to support the design of spillways by a direct mathematical approach instead of trial-and-error methods.

First, a two-dimensional model is formulated to determine the free surface and the discharge for a stationary, incompressible, homogeneous, non-viscous and irrotational flow over a fixed spillway. The flow satisfies the Laplace equation and the Bernoulli equation (potential flow). An important feature of the model is that it can be extended to design the spillway structure when the spillway is not fixed but the pressure on the spillway is described by a cavitation criterion.

Next, the continuous model is discretized by the boundary element method (BEM). We use a non-linear programming algorithm to calculate the pressures and the shape of the spillway. A computer-aided design package is developed on a PC using the equations describing the free surface, the BEM and standard optimization techniques. The input and output of the model are realized using graphical routines. Finally, we discuss the convergence and the computation time of the algorithms.

KEY WORDS **Boundary element method Computer aided design Optimization**

1. INTRODUCTION

The objective of this paper is to study the cavitation damage on the shape of a spillway. First, we formulate and solve the model which describes the location of the free surface and the discharge of flows over weirs and spillways. The model is restricted to stationary potential flows. Secondly, we use the potential flow solution to study the cavitation damage. If there is cavitation, the shape will be changed in order to prevent damage as much as possible. Thus the model calculates the free surface, the flow and the discharge and also helps to study cavitation.

In recent years much research has been carried out to solve stationary potential flows over weirs. Chan *et al.*,[1] Washizu and Nakayama[2] and Dierch *et al.*[3] solved the problem by using the

0271–2091/91/150625–17$08.50

Received April 1989
Revised November 1990

finite element method (FEM) to discretize the Laplace equation which describes the potential flow. O'Carroll and Toro[4,21] used the variational approach together with the FEM and a Kantorovisch computational method to find the solution.

We will discretize the model given in Section 2 with the boundary element method (BEM). Aitchison[5] solved another free surface problem with the BEM. In Section 3 we give the advantages of the BEM compared with the FEM. It is also important that we use a model with a decreasing free surface and a uniform inflow.

The outline of the paper is as follows. Section 2 contains the physical assumptions and the continuous model equations found by these assumptions. Section 3 explains the BEM and presents the discrete model equations found by the BEM. Section 4 presents the dimensionless model obtained from the discrete equations of Section 3 and the computer programme structure of this model. In Section 5 we give results for a particular weir. In particular, the influence of the choice of the boundary elements is studied. Section 6 gives the values used to study cavitation. First, we give the method by which these values can be calculated from the potential flow solution. Next, we give two cavitation criteria. Finally, a suggestion to extend the model to an optimal spillway design model is given. In Section 7 we give some final remarks.

2. PHYSICAL ASSUMPTIONS AND THE CONTINUOUS MODEL EQUATIONS

Suppose we have a large reservoir of water. Water flows over a weir in the reservoir. Furthermore, we suppose that the flow can be described by velocities, the location of the free surface and the discharge. The discharge is the volume of water that flows in the reservoir every second. The flow can be calculated from the equations given in this section. It is necessary to impose certain conditions upon the flow to derive these equations. The equations and conditions will be taken on a two-dimensional domain Ω around the weir (see Figure 1).

First, we assume that the flow out of the reservoir is time-independent. This assumption means that the water level of the reservoir, the stagnation level, does not change in time and the potential energy of the reservoir is therefore time-independent. This assumption holds, of course, only in the domain Ω. In the reservoir at a large distance from the weir the velocity will be zero and so the velocity on the stagnation level will also be zero. It is necessary that the free surface level at the inlet of the domain Ω be lower than the stagnation level, since there is flow into the domain and therefore loss of potential energy.

Furthermore, we assume that the flow is incompressible, homogeneous, non-viscous and irrotational. This means that we have a steady potential flow satisfying the Laplace differential equation and the Bernoulli equation in Ω. Since the flow is incompressible, the discharge Q is constant through the whole domain. The empirical constant H_0 is defined as the distance between the stagnation level and a specified horizontal level in the reservoir. The part of the reservoir from this specified level to the bottom is taken out of the domain Ω, because there the velocities are small and the influence of this part on the outflow is negligible. We choose a co-ordinate system with the origin above the inlet of the domain Ω and on the stagnation level, the positive x downwards and the positive y to the right. The atmospheric pressure is taken as zero. In this co-ordinate system the Bernoulli equation can be given by

$$p+\tfrac{1}{2}\rho|v|^2-\rho g x=0, \tag{1}$$

where p is the pressure, v is the velocity, ρ is the density constant and g is the gravity constant. In this equation we have found the Bernoulli constant by using the Bernoulli equation on the stagnation level, because there the velocity is zero and the (atmospheric) pressure is also zero.

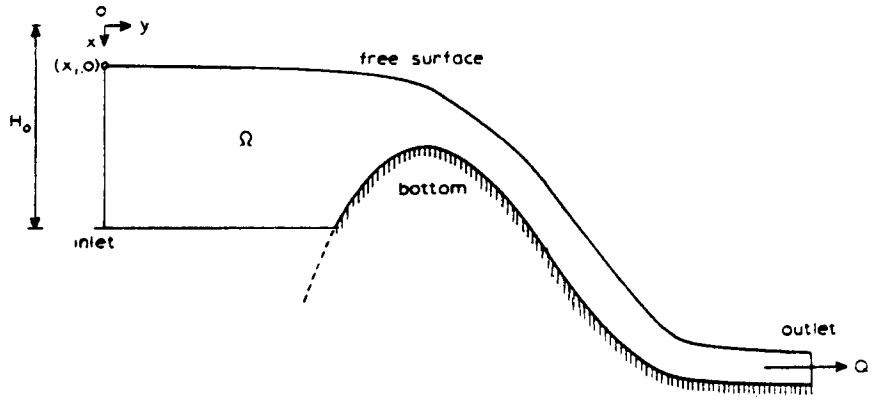

Figure 1. Domain of the continuous two-dimensional model

Now we define a streamfunction $\Psi = \Psi(x, y)$ with

$$\frac{\partial \Psi}{\partial x} = -v_y \quad \text{and} \quad \frac{\partial \Psi}{\partial y} = v_x, \tag{2}$$

where v_x is the velocity in the x-direction and v_y is the velocity in the y-direction.

Using the incompressibility and the irrotationality of the flow, we can formulate Laplace's equation as

$$\frac{\partial^2 \Psi}{\partial x^2} + \frac{\partial^2 \Psi}{\partial y^2} = 0. \tag{3}$$

The lines on which Ψ is constant are called streamlines and the direction of the velocity is tangent to the streamline. Since particles follow a streamline, we can assume that the bottom and the free surface of the domain are both streamlines. The definition of the discharge through a vertical line segment gives a relation between Ψ and the discharge,

$$Q = \int_{s(y)}^{b(y)} v_y \, dx = -\int_{s(y)}^{b(y)} \frac{\partial \Psi}{\partial x} dx = \Psi(s(y), y) - \Psi(b(y), y) = \Psi_f - \Psi_b, \tag{4}$$

where $s(y)$ is a function for the free surface, $b(y)$ is a function for the bottom, Ψ_f is the constant Ψ on the free surface and Ψ_b is the constant Ψ on the bottom. Now we choose $\Psi_f = Q + K$ and $\Psi_b = K$ with K constant. The constant value K is a translation factor in the solution of the problem and can be taken as zero. Thus we have

$$\Psi_f = Q \quad \text{and} \quad \Psi_b = 0. \tag{5}$$

The velocity along the boundary of the domain can be given by $\partial \Psi / \partial n$, with n the outward normal vector on the boundary. Another condition on the free surface is found from the Bernoulli equation (1) using $p = p_{atm} = 0$ and $v = \partial \Psi / \partial n$:

$$\left(\frac{\partial \Psi}{\partial n}\right)^2 - 2gx = 0. \tag{6}$$

This equation gives a simple relation between the location of the free surface and the velocity on that surface. We assume that the upstream section of our domain is large enough to satisfy

uniform flow through the inlet and we also assume that the flow through the outlet is horizontal. Horizontal flow means that the vertical velocities are zero. Furthermore, uniform flow is a horizontal flow with constant horizontal velocities. From these assumptions we obtain at the outlet the boundary condition

$$\frac{\partial \Psi}{\partial n}=0, \tag{7}$$

and at the inlet the conditions

$$\Psi=Q\frac{H_0-x}{H_0-x_1} \tag{8a}$$

$$\frac{\partial \Psi}{\partial n}=0, \tag{8b}$$

with $(x_1, 0)$ the position of the free surface at the inlet. Condition (8a) agrees with the conditions in (5) for $x=x_1$ and $x=H_0$. To determine the discharge, we use a direct relation between this discharge and x_1,

$$Q=(H_0-x_1)(2gx_1)^{1/2}, \tag{9}$$

which can be found by using equation (1) for the point $(x_1, 0)$ with $v=Q/(H_0-x_1)$ and $p=p_{\text{atm}}$. The equation for v is obtained from the uniform flow through the inlet. If x_1 increases from zero to $\frac{1}{3}H_0$, the discharge Q increases from zero to $Q_{\max}=H_0\sqrt{[(8/27)gH_0]}$, and if x_1 increases from $\frac{1}{3}H_0$ to H_0, then Q decreases from $Q_{\max}$ to zero. In the case of a flow in a channel without a weir there is a constant water level $\bar{x}=\frac{1}{3}H_0$ through the whole domain and there is a constant horizontal velocity through the whole domain (uniform flow). If there is a weir, the water level at the inlet will always be higher than $\frac{1}{3}H_0$. Therefore we assume that x_1 is restricted to the interval $(0, \frac{1}{3}H_0)$. This yields the extra condition

$$0\leqslant x_1\leqslant \tfrac{1}{3}H_0. \tag{10}$$

The last assumption is that we restrict the model to problems where the free surface function $s(y)$ is an increasing function. Thus the surface descends from the inlet until the outlet. This gives

$$\frac{\mathrm{d}s(y)}{\mathrm{d}y}\geqslant 0. \tag{11}$$

This assumption is introduced to avoid a solution with waves on the free surface. The assumption is valid for low weirs in a channel[6, 7] based on the hydrostatic pressure distribution. For spillways the assumption is not proven but there has never been found a spillway with an increasing free surface.

Taking all the equations together, we obtain the continuous model:

$$\frac{\partial^2 \Psi}{\partial x^2}+\frac{\partial^2 \Psi}{\partial y^2}=0 \qquad \text{(in } \Omega\text{)}, \tag{12a}$$

$$\Psi=0 \qquad \text{(on the bottom)}, \tag{12b}$$

$$\Psi=Q \qquad \text{(on the free surface)}, \tag{12c}$$

$$\frac{\partial \Psi}{\partial n}=0 \qquad \text{(at the outlet)}, \tag{12d}$$

$$\frac{\partial \Psi}{\partial n}=0 \qquad \text{(at the inlet)}, \tag{12e}$$

$$\Psi=Q\frac{H_0-x}{H_0-x_1} \qquad \text{(at the inlet)}, \tag{12f}$$

$$\left(\frac{\partial \Psi}{\partial n}\right)^2-2gx=0 \qquad \text{(on the free surface)}, \tag{12g}$$

$$Q=(H_0-x_1)(2gx_1)^{1/2} \qquad \text{(at the point } (x_1,0)\text{)}, \tag{12h}$$

$$0\leqslant x_1\leqslant \tfrac{1}{3}H_0, \tag{12i}$$

$$\frac{\mathrm{d}s(y)}{\mathrm{d}y}\geqslant 0 \qquad \text{(on the free surface)}, \tag{12j}$$

3. DISCRETIZATION OF THE MODEL USING THE BOUNDARY ELEMENT METHOD (BEM)

One popular discretization method for potential flows is the finite element method (FEM), where the total domain is divided into elements.[8-10] The FEM is frequently applied to many problems since a lot of the elements are independent of each other and therefore the matrices found by the FEM contain many zeros. However, for free surface problems the FEM discretization gives difficulties. Suppose that the location of the free surface in such a problem is found by an iteration process. The elements near the free surface cannot be constant during these iterations so that the variation of these elements makes the discretization complicated.[11]

At the end of the 1970s and the beginning of the 1980s Brebbia studied another discretization method for potential problems, the boundary element method (BEM).[12-14] This method needs only a discretization of the boundary of the domain, and when the solution on the boundary has been calculated, the solution inside the domain can also be calculated. The elements of the BEM are not independent and therefore the matrices obtained by this method contain fewer zeros. However, the dimension of the matrices is smaller than the dimension of the matrices obtained by the FEM and the discretization of the free surface is much easier. For this reason we have chosen to apply the BEM. However, before we can use the BEM discretization we need a continuous model with all equations and conditions on the boundary of the domain. The Laplace equation, valid in the entire domain, can be replaced by an equivalent integral equation on the boundary. The equation is based on Green's second theorem:[14, 15]

$$\int\int_S (\phi\nabla^2\phi^*-\phi^*\nabla^2\phi)\,\mathrm{d}s=\oint_C\left(\phi\frac{\partial\phi^*}{\partial n}-\phi^*\frac{\partial\phi}{\partial n}\right)\mathrm{d}c, \tag{13}$$

where S is a closed domain, C is the boundary of the domain, ϕ is a function satisfying the Laplace equation, ϕ^* is a free function, ∇^2 is the Laplace operator and n is the outward normal vector (see Figure 2). The function ϕ is replaced by Ψ and for ϕ^* we choose the fundamental solution for the two-dimensional case,[14]

$$\phi^*=\log\left(\frac{1}{|\boldsymbol{\tau}-\mathbf{r}|}\right), \tag{14}$$

where $\mathbf{r}$ is a vector from the origin O to a fixed point A on C and $\boldsymbol{\tau}$ is a vector from the origin O to a free point on C (see Figure 2). The fundamental solution, which is a function of $\boldsymbol{\tau}$, satisfies Laplace equation for every $\boldsymbol{\tau}\neq\mathbf{r}$.

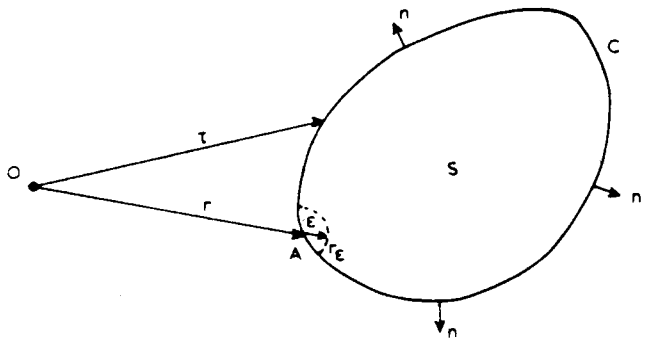

Figure 2. Boundary to illustrate the Green equation

It can now be proved[15, 16] that (13) is equivalent to

$$\int_C \left[\Psi(\tau) \frac{\partial}{\partial n} \log\left(\frac{1}{|\tau - \mathbf{r}|}\right) - \log\left(\frac{1}{|\tau - \mathbf{r}|}\right) \frac{\partial \Psi(\tau)}{\partial n} \right] dc + \alpha(\mathbf{r})\Psi(\mathbf{r}) = 0, \tag{15}$$

with $\alpha(\mathbf{r}) = 0$ if $\mathbf{r}$ is the vector to a point not in S, $\alpha(\mathbf{r}) = \alpha$ if $\mathbf{r}$ is the vector to a point on C $(0 \leqslant \alpha \leqslant 2\pi)$ and $\alpha(\mathbf{r}) = 2\pi$ if $\mathbf{r}$ is the vector to a point in S. If the boundary is smooth, we have $\alpha = \pi$. The basic elements of the proof are: take a point A on C and remove a half-circle area with centre A and small radius ε from S; for the remaining area, (13) is calculated and, finally, the limit $\varepsilon \to 0$ is taken in the obtained expression. Sneddon[15] proves the equation for an interior point. The proof for a boundary point is similar.

We are now able to discretize the boundary of Figure 1 by the BEM using linear (first-order) elements (line segments). We choose $m+1$ nodal points on the boundary with the first nodal point at the highest point at the inlet, and from this point we number the nodal points in a clockwise direction (see Figure 3). Then the nodal points are connected by m linear elements so that a closed approximation of the real contour is obtained. The centre point of an element is called an element point.

The notations for the nodal points and the element points are given in Figure 3. Now we choose Ψ and $\partial\Psi/\partial n$ constant on each element. This choice is recommended by Romate[17] who suggests taking the order of an element exactly one degree higher than the Ψ and the $\partial\Psi/\partial n$ on that element. Thus in (15) Ψ and $\partial\Psi/\partial n$ are constant on each element and the remaining integrals are defined by

$$a_{ij} = \int_{C_j} \frac{\partial}{\partial n} \log\left(\frac{1}{r_{ij}}\right) dc + \pi\delta_{ij}, \quad \text{with } \delta_{ij} = \begin{cases} 1 & \text{if } i = j, \\ 0 & \text{if } i \neq j, \end{cases} \tag{15a}$$

$$b_{ij} = \int_{C_j} \log\left(\frac{1}{r_{ij}}\right) dc, \tag{15b}$$

where C_j indicates element j and r_{ij} is the distance between element point i and a free point on element j $(i = 1 \ldots m, j = 1 \ldots m)$. It is obvious that we cannot use definition (15) for higher-order elements since Ψ and $\partial\Psi/\partial n$ are not constant. In this case the integrals in (15) can only be solved numerically.

With (15a, b) equation (15) gives the matrix expression

$$\mathbf{A}\Psi = \mathbf{B}\Psi_n, \tag{16}$$

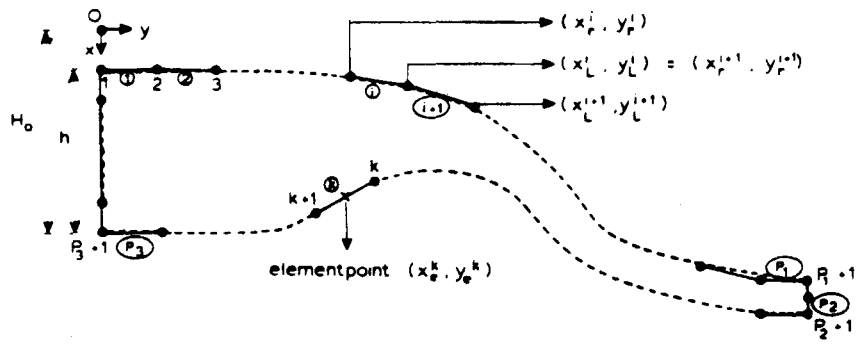

Figure 3. Discretization of the boundary with linear elements

where $\mathbf{A}$ is an $m \times m$ matrix with coefficients a_{ij}, $\mathbf{B}$ is an $m \times m$ matrix with coefficients b_{ij}, $\boldsymbol{\Psi}$ is an m-vector with components Ψ^j and $\boldsymbol{\Psi}_n$ is an m-vector with components $\partial\Psi^j/\partial n$ ($j=1 \ldots m$). For a_{ij} and b_{ij} it is possible to give analytical expressions. The expressions are given here for three different cases. First, for $i=1 \ldots m$ and $j=1 \ldots m$ we define

$$L_i=[(x_r^i-x_1^i)^2+(y_r^i-y_1^i)^2]^{1/2}, \tag{17a}$$

$$\alpha_i=L_i^2, \tag{17b}$$

$$\beta_{ij}=2[(x_r^j-x_1^j)(x_1^j-x_e^i)+(y_r^j-y_1^j)(y_1^j-y_e^i)], \tag{17c}$$

$$\gamma_{ij}=[(x_1^j-x_e^i)^2+(y_1^j-y_e^i)^2], \tag{17d}$$

$$\nu_{ij}=[-(y_r^j-y_1^j)(x_1^j-x_e^i)+(x_r^j-x_1^j)(y_1^j-y_e^j)], \tag{17e}$$

where (x_r^i, y_r^i), (x_1^i, y_1^i) are the nodal points and (x_e^i, y_e^i) are the element points of element i (see Figure 3). The expressions in the three different cases for a_{ij} and b_{ij} are

(i) expressions for the diagonal coefficients ($i=j$)

$$a_{ij}=\pi,$$

$$b_{ij}=L_i[1-\log(L_i/2)]; \tag{18a}$$

(ii) expressions for the coefficients with $\nu_{ij}=0$ ($i \neq j$)

$$a_{ij}=0$$

$$b_{ij}=L_j+\frac{1}{4L_j}[-(2\alpha_j+\beta_{ij})\log(\alpha_{ij}+\beta_{ij}+\gamma_{ij})+\beta_{ij}\log(\gamma_{ij})]; \tag{18b}$$

(iii) expressions for the coefficients with $\nu_{ij} \neq 0$ ($i \neq j$)

$$a_{ij}=\tan^{-1}\left(\frac{2\alpha_j+\beta_{ij}}{2\nu_{ij}}\right)-\tan^{-1}\left(\frac{\beta_{ij}}{2\nu_{ij}}\right),$$

$$b_{ij}=L_j+\frac{1}{4L_j}[-(2\alpha_j+\beta_{ij})\log(\alpha_{ij}+\beta_{ij}+\gamma_{ij})+\beta_{ij}\log(\gamma_{ij})]-\frac{\nu_{ij}}{L_j}a_{ij}. \tag{18c}$$

As mentioned before, the expressions above can only be derived for linear elements. For higher-order elements there is also a matrix expression like (16) but the dimension of this matrix is larger and the derivation of this expression costs more effort.[14]

It is convenient to introduce two vectors **x** and **y** (dimension $m+1$) with

$$x_1 = x_1^m = x_r^1, \qquad y_1 = y_1^m = y_r^1,$$
$$x_i = x_1^{i-1} = x_r^i, \qquad y_i = y_1^{i-1} = y_r^i, \qquad i = 2 \ldots m,$$
$$x_{m+1} = x_1, \qquad y_{m+1} = y_1, \tag{19}$$

where the indices $1 \ldots p_1+1$ correspond to the free surface co-ordinates, the indices $p_1+1 \ldots p_2+1$ to the outlet co-ordinates, the indices $p_2+1 \ldots p_3+1$ to the bottom co-ordinates and the indices $p_3+1 \ldots m+1$ to the inlet co-ordinates. In our discrete model definition we choose the vector **x** constant in the bottom components and the vector **y** constant in all components. Moreover, we define a fixed number of elements, each of equal size, at the inlet and at the outlet which are fixed by the equations

$$x_{p_3+1+i} = x_{p_3+1} - i\,\frac{x_{p_3+1} - x_1}{m - p_3}, \qquad i = 1 \ldots m - p_3, \tag{20a}$$

$$x_{p_2+1-i} = x_{p_2+1} - i\,\frac{x_{p_2+1} - x_{p_1+1}}{p_2 - p_1}, \qquad i = 1 \ldots p_2 - p_1. \tag{20b}$$

Thus the vector $\mathbf{X} = (x_1, x_2, \ldots, x_{p_1+1})$ contains the remaining free components, which determine the free surface. The x-components on the inlet and on the outlet, given by (20), depend on **X**. Using (12) and the assumptions of the last section, we obtain the discrete model:

$$\mathbf{A\Psi} = \mathbf{B\Psi}_n \quad (\mathbf{A(X)} \text{ and } \mathbf{B(X)} \text{ given by (18)}), \tag{21a}$$
$$\Psi^i = 0 \qquad \text{for } i = p_2+1 \ldots p_3, \tag{21b}$$
$$\Psi^i = Q \qquad \text{for } i = 1 \ldots p_1, \tag{21c}$$
$$\Psi_n^i = 0 \qquad \text{for } i = p_1+1 \ldots p_2, \tag{21d}$$
$$\Psi_n^i = 0 \qquad \text{for } i = p_3+1 \ldots m, \tag{21e}$$
$$\Psi^i = Q\,\frac{i - p_3 - 0{\cdot}5}{m - p_3} \qquad \text{for } i = p_3+1 \ldots m, \tag{21f}$$
$$(\Psi_n^i)^2 - g(x_i + x_{i+1}) = 0 \qquad \text{for } i = 1 \ldots p_1, \tag{21g}$$
$$Q = (H_0 - x_1)(2gx_1)^{1/2}, \tag{21h}$$
$$0 \leqslant x_1 \leqslant \tfrac{1}{3}H_0, \tag{21i}$$
$$x_i \leqslant x_{i+1} \qquad \text{for } i = 1 \ldots p_1. \tag{21j}$$

To find the solution of this model, we have to solve the unknowns **X**, Q, Ψ^i for $i = p_1+1 \ldots p_2$, Ψ^i for $i = p_3+1 \ldots m$, Ψ_n^i for $i = 1 \ldots p_1$ and Ψ_n^i for $i = p_2+1 \ldots p_3$ from the non-linear equations (21). This can be done if we transform (21) to a dimensionless model that can be solved using a non-linear optimization routine and a Gauss elimination routine.

4. DIMENSIONLESS MODEL AND PROGRAMME STRUCTURE

Equations (21) are made dimensionless with the length H_0 and the time $(H_0/g)^{1/2}$. This is important since the dimensionless variables give equal-weighted equations which are necessary to achieve a good result in the optimization routine. The dimensionless variables in the remainder of

this paper have the same notation as the variables used before. Equations (21) are transformed to the following dimensionless equations:

$$\mathbf{A\Psi}=(\mathbf{B}-\mathbf{C})\mathbf{\Psi}_n, \quad \text{with } c_{ij}=L_j\log(H_0) \quad \text{for all } i=1\ldots m, \tag{22a}$$

$$\Psi^i=0 \quad \text{for } i=p_2+1\ldots p_3, \tag{22b}$$

$$\Psi^i=Q \quad \text{for } i=1\ldots p_1, \tag{22c}$$

$$\Psi_n^i=0 \quad \text{for } i=p_1+1\ldots p_2, \tag{22d}$$

$$\Psi_n^i=0 \quad \text{for } i=p_3+1\ldots m, \tag{22e}$$

$$\Psi^i=Q\frac{i-p_3-0{\cdot}5}{m-p_3} \quad \text{for } i=p_3+1\ldots m, \tag{22f}$$

$$(\Psi_n^i)^2-(x_i+x_{i+1})=0 \quad \text{for } i=1\ldots p_1, \tag{22g}$$

$$Q=(1-x_1)(2x_1)^{1/2}, \tag{22h}$$

$$0\leqslant x_1\leqslant\tfrac{1}{3}, \tag{22i}$$

$$x_i\leqslant x_{i+1} \quad \text{for } i=1\ldots p_1. \tag{22j}$$

We subdivide matrix **A** (and in a similar manner **B** and **C**) into four submatrices

$$\mathbf{A}=[\mathbf{A1}\ \ \mathbf{A2}\ \ \mathbf{A3}\ \ \mathbf{A4}], \tag{23}$$

where **A1** contains the columns $1\ldots p_1$ of **A**, **A2** the columns $p_1+1\ldots p_2$, **A3** the columns $p_2+1\ldots p_3$, **A4** the remaining columns. Using (22a–e), we obtain the system

$$\mathbf{F(X)\Phi(X)=G(X)}, \tag{24}$$

with

$$\mathbf{F(X)}=[-\mathbf{B1}+\mathbf{C1}\ \ \mathbf{A2}\ \ -\mathbf{B3}+\mathbf{C3}\ \ \mathbf{A4}] \quad (m\times m),$$

$$\mathbf{\Phi}^{\mathrm{T}}(\mathbf{X})=[\Psi_n^1\ldots\Psi_n^{p_1},\ \Psi^{p_1+1}\ldots\Psi^{p_2},\ \Psi_n^{p_2+1}\ldots\Psi_n^{p_3},\ \Psi^{p_3+1}\ldots\Psi^m] \quad (m),$$

$$\mathbf{G}^{\mathrm{T}}(\mathbf{X})=\left[-Q\sum_{j=1}^{p_1}Al_{1j},\ldots,-Q\sum_{j=1}^{p_1}Al_{mj}\right] \quad (m).$$

If we start with an initial vector **X**, we obtain an iteration process with, in each iteration, **X** known from the preceding iteration. Thus in each iteration the vector $\mathbf{\Phi(X)}$ can be calculated with (24) and Q can be calculated with (22h). We use (22g) in the object function definition of the optimization model and the remaining relations, (22f, i, j), are the constraints. The model is formulated as

$$\min_{\mathbf{X}}\sum_{i=1}^{p_1}(h_i)^2=\sum_{i=1}^{p_1}[\Phi_i(\mathbf{X})^2-(x_i+x_{i+1})]^2,$$

subject to

$$\Phi_i(\mathbf{X})-Q\frac{i-p_3-0{\cdot}5}{m-p_3}=0 \quad \text{for } i=p_3+1\ldots m,$$

$$0\leqslant x_1\leqslant\tfrac{1}{3}$$

$$x_i-x_{i+1}\leqslant 0 \quad \text{for } i=1\ldots p_1, \tag{25}$$

where $\mathbf{\Phi}$ and Q can be calculated by (24) and (22h) for a given **X**.

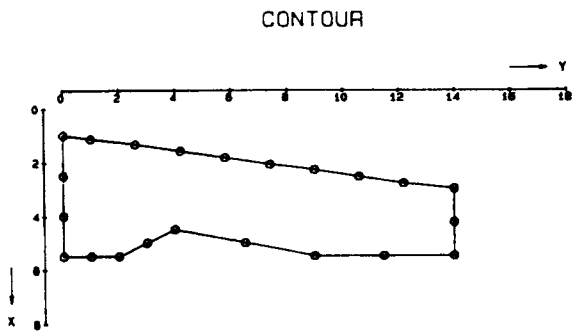

Figure 4. Initial values for the free surface (case I)

Table I. Results for different numbers of elements in the inlet and outlet ((dim) means dimensionless)

Case	Number of elements		Q	$\max_i \lvert h_i \rvert$	$\min_X \sum_{i=1}^{p_1} (h_i)^2$	Time
	Inlet	Outlet	($m^2 s^{-1}$)	(dim)	(dim)	(s)
Ia	3	2	19·288	0·02086	0·00137	175
Ib	4	2	19·345	0·00758	0·00015	170
Ic	4	3	19·358	0·00575	0·00012	150
Id	5	3	19·351	0·00397	0·00004	185
Ie	6	3	19·350	0·00555	0·00009	185
If	7	3	19·343	0·00479	0·00007	203

An optimization routine in Fortran is developed to calculate the solution of (25). This routine contains the standard optimization routine NCONF from the IMSL library, which uses the successive quadratic programming algorithm and a finite difference gradient to solve (25) for a given start value[18] and the standard Gauss elimination routine F04ARF from the NAG library to solve (24). The routine converges to the solution for a good initial value of $\mathbf{X}$. When the solution has been found, Q and the vector $\mathbf{\Phi}$ are of course also available. The vector $\mathbf{\Phi}$ contains the remaining values of $\mathbf{\Psi}$ and $\mathbf{\Psi}_n$ on the boundary. With $\mathbf{\Psi}$ and $\mathbf{\Psi}_n$ on the boundary and the position of the boundary we can also calculate $\mathbf{\Psi}$ at every point in the domain.[12] The optimization routine is part of a larger programme which makes it possible to manipulate boundaries on the screen and on disc (graphical editing).

5. COMPUTATIONS FOR A PARTICULAR WEIR AND THE INFLUENCE OF THE ELEMENT AND DOMAIN CHOICE

In this section we first study the effect of the number of elements in the inlet and outlet on the solution. We then study the behaviour of the solution if we enlarge the upstream and downstream sections.

A particular weir with the initial free surface is given in Figure 4. For $H_0 = 5{\cdot}5$ we have made six computations, with in each case a different number of elements in the inlet and outlet. Table I

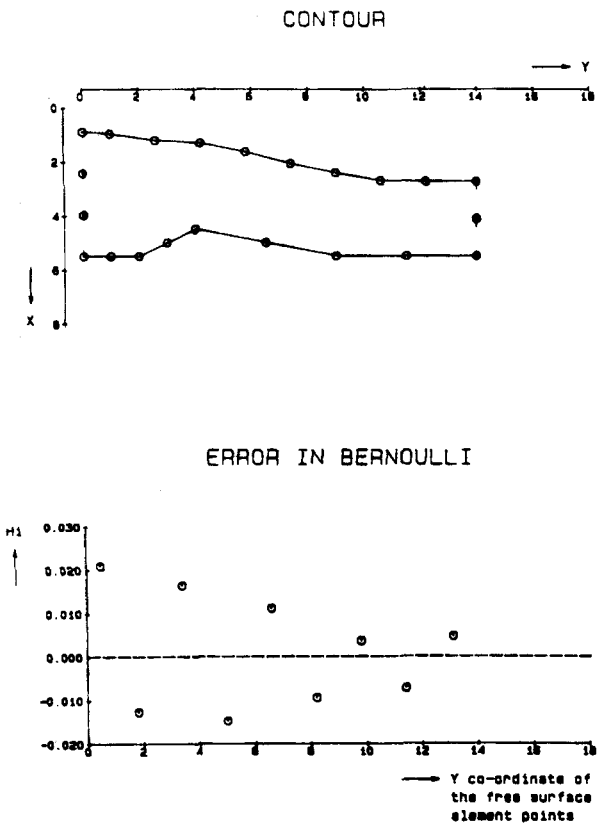

Figure 5. Contour and Bernoulli errors (case Ia)

shows the number of elements, the discharge Q, the maximum absolute error in Bernoulli's constant, the value of the object function and the computation time (on an Olivetti M24 SP) for each case.

The object function and the maximal absolute error in Bernoulli in Table I are smaller for more elements in the inlet and outlet. Thus we can conclude that more elements in the inlet and outlet improve the location of the free surface since Bernoulli is better satisfied (compare Figure 5 with Figure 6). A large improvement is especially obtained if we increase the number of elements used in case Ia. The discharge is almost the same in the six cases. When we have chosen a sufficient number of elements in the inlet and outlet we obtain a relatively small object function. An improvement by using more elements of the object function is impossible. Generally, a problem with more elements needs more computation time in each iteration since the matrices are larger. Thus it is useful to take more elements only if this leads to a relatively large improvement in the object function or an improvement in the computation time.

For the same weir, but now with $H_0 = 5{\cdot}6$, we study the solution for different upstream and downstream sections. The length of the upstream section is U and the length of the downstream section is D (see Figure 7). Table II shows the discharge, the maximum absolute error in Bernoulli's value and the value of the object function for different U and D.

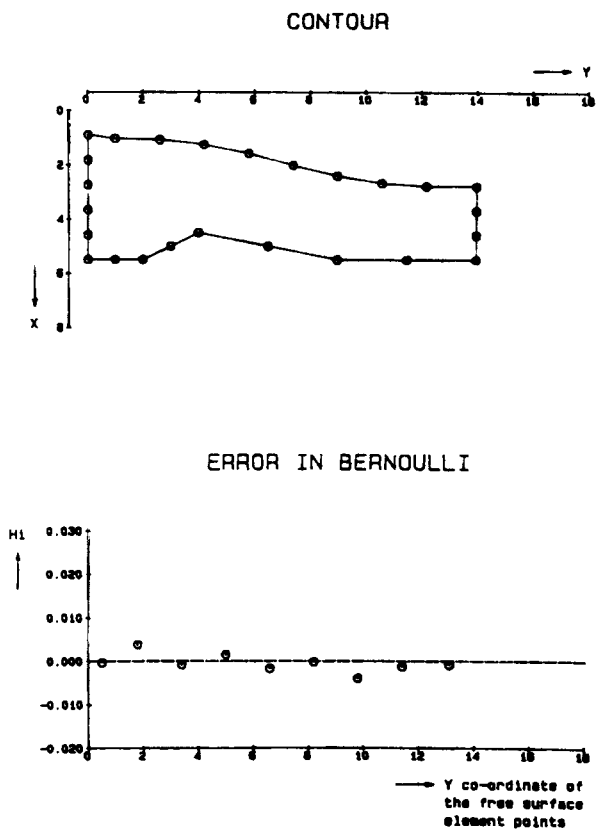

Figure 6. Contour and Bernoulli errors (case Id)

Table II. Results for different upstream and downstream sections

Case	U (m)	D (m)	Q ($m^2\,s^{-1}$)	$\max_i \lvert h_i \rvert$ (dim)	$\min_x \sum_{i=1}^{p_1} (h_i)^2$ (dim)
IIa	2	5	19·993	0·00979	0·00017
IIb	3	5	20·070	0·00682	0·00018
IIc	4	5	20·059	0·00887	0·00018
IId	4	6	20·069	0·03719	0·00227
IId1	4	6	20·103	0·00974	0·00017
IIe	4	7	20·115	0·01076	0·00016

The table shows, except in case IId, that the solutions do not differ very much. The result of case IId in Figure 8 shows a relatively large error in Bernoulli's constant in the last element on the free surface. This is caused by the small length of this element, since the element point lies near the corner point on the boundary. In this corner point not only is the boundary discontinuous but also the velocity; hence there is a large error in Bernoulli's constant. In case IId1 we have changed

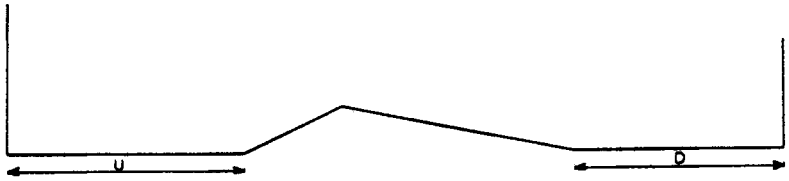

Figure 7. Definition of upstream length U and downstream length D

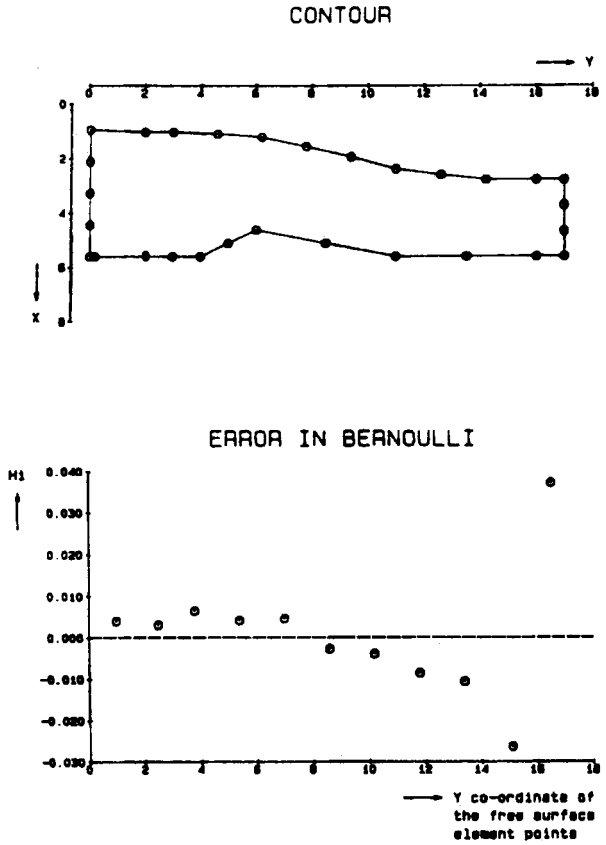

Figure 8. Contour and Bernoulli errors (case IId)

the size of the elements on the free surface to obtain a large corner element. Figure 9 shows the improvement in the object function and the maximum error in Bernoulli's constant. Figure 9 also shows that the largest error in Bernoulli's constant is near the second element on the free surface. This element is shorter than the other elements on the surface. Finally, we remark that a better result is obtained by using free surface elements with equal size and by avoiding small corner elements.

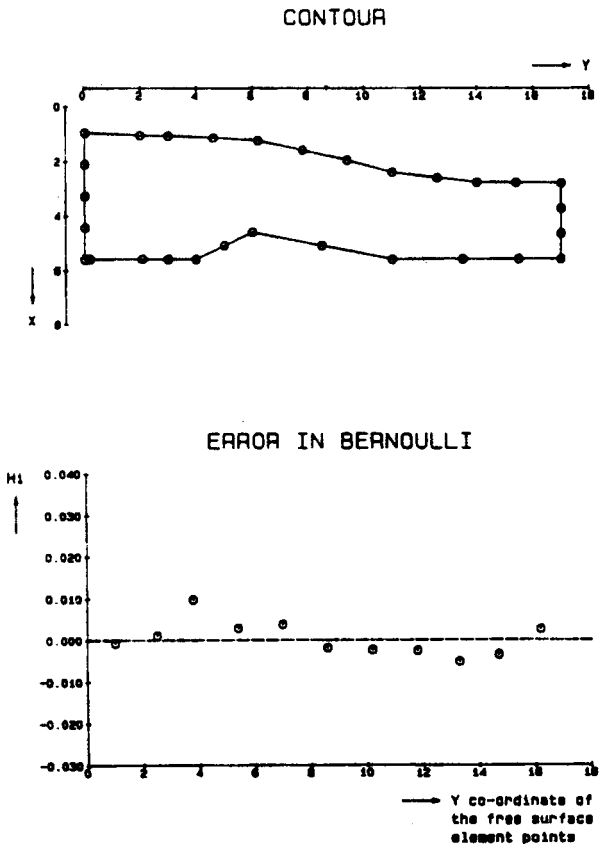

Figure 9. Contour and Bernoulli errors (case IId1)

6. CAVITATION CRITERION

The most important aspect of a flow over a spillway is the detection of cavitation on the spillway shape, since cavitation can result in damage on the spillway. In general, cavitation cannot always be avoided, but we can control the point on the shape of the spillway where cavitation starts by changing the shape. The design of the shape is better when this point is situated farther away from the crest of the spillway.

The real velocity on the bottom is zero. Therefore a boundary layer exists, which grows along the shape and in which the velocity drops from the mean velocity at the top of the layer to zero on the bottom. For the flow over the boundary layer we take the potential flow found from the optimization model (see Figure 10).

The thickness of the boundary layer is found from[19]

$$\frac{\delta(x)}{x} = 0{\cdot}37 \left(\frac{U(x)}{v_f}\right)^{-0{\cdot}2}, \tag{26}$$

where $\delta(x)$ is the thickness function, x is the distance from the crest of the spillway, $U(x)$ is the mean velocity of the potential flow and v_f is the kinetic viscosity of water (see Figure 10). In the discrete model the distance x to an element point can be derived from the size of the elements on

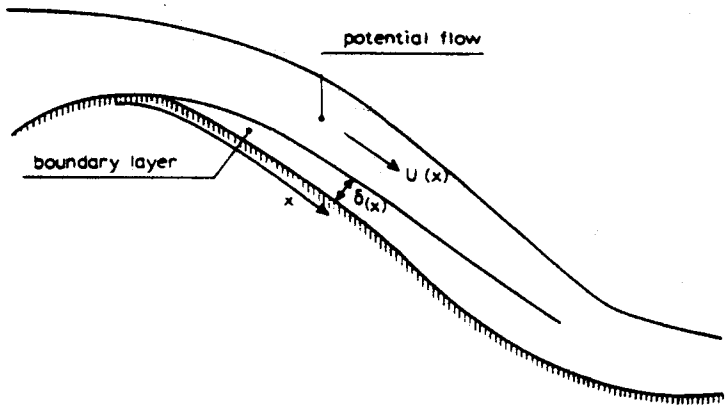

Figure 10. Boundary layer on the spillway

the shape, and $U(x)$ at each element point can be derived from the known discharge, the angle of the element and the height of the domain above the element point. If the solution of the potential flow is known, we can calculate $\delta(x)$ at every element point on the shape.

The cavitation can be measured with different criteria, of which two are given in this section. One uses the Holl and the Thoma values and the other uses the Gal'perin and the Thoma values. First we give the definition of these values[20] and next we present the criteria.

The Thoma value $K(x)$ is defined as

$$K(x)=\frac{p(x)+p_{\text{atm}}-p_{\text{v}}}{0{\cdot}5\rho U(x)^2}, \tag{27}$$

where $p(x)$ is the pressure on the bottom of the potential flow, p_{atm} is the atmospheric pressure and p_{v} is the vapour pressure. The pressure $p(x)$ is found for each element point from the solution of the potential flow, and p_{atm} and p_{v} are known constants.

Before we introduce the Gal'perin value and the Holl value we first define the velocity at a small distance y from the real bottom:

$$u_y(x)=\left(\frac{y}{\delta(x)}\right)^{0{\cdot}2} U(x). \tag{28}$$

(In our calculations we use $y=0{\cdot}01$ m.) The definition of the Gal'perin value is

$$\sigma_{\text{G}}(x)=1{\cdot}76\left(\frac{u_y}{U(x)}\right)^2 \tag{29a}$$

and the definition of the Holl value is

$$\sigma_{\text{H}}(x)=1{\cdot}415\left(\frac{y}{\delta(x)}\right)^{0{\cdot}4}. \tag{29b}$$

With the solution of the potential model we can calculate (27) and (29) at every element point on the shape. The variable x is found from a summation of the size of the elements, starting with the element on the top of the weir. We define two different values to detect cavitation:

$$\Delta_{\text{G}}(x)=K(x)-\sigma_{\text{G}}(x), \tag{30a}$$

$$\Delta_{\text{H}}(x)=K(x)-\sigma_{\text{H}}(x). \tag{30b}$$

These values can be determined for every element point on the shape. There is cavitation at the element points where Δ_G or Δ_H is negative. The value σ_G is in general larger than the value σ_H. Therefore the definition of Gal'perin detects cavitation sooner and so the shape is more restricted. Low weirs have a shape with all Δs positive. In that case we will try to find a shape with the Δs as small as possible, because a shape with a large Δ is expensive. Generally, it is impossible to find a shape for a high spillway with a Δ which is positive at all element points. Subsequently, we will try to find a shape with element points with cavitation far away from the spillway crest and the remaining positive Δs as small as possible.

It is difficult to extend the model (22) to a model where not only the free surface is unknown but in which also a part of the free spillway shape is unknown. The conditions to determine the position of this free part on the spillway shape cannot easily be given, because a simple equation such as Bernoulli's on the free surface is not available. We suggest that only the part on the shape where we do not want cavitation is taken as free and that the volume of the spillway is minimized with all Δs positive. Suppose there are two fixed nodal points with indices $l_{\min}$ and $l_{\max}$ on the shape. The free nodal points on the shape are denoted with index l ($l_{\min} < l < l_{\max}$ and $x_{l_{\min}} > x_{l_{\max}}$). Furthermore, we can assume that the free part of the shape decreases for increasing y. The vector $\mathbf{X}$ of Section 4 can now be extended to the vector $\mathbf{Z} = (\mathbf{X}, x_{l_{\min}+1}, x_{l_{\min}+2}, \ldots, x_{l_{\max}-2}, x_{l_{\max}-1})$ and the model can be given as

$$\min \sum_{l=l_{\min}+1}^{l_{\max}} \tfrac{1}{2}(y_{l-1}-y_l)(2x_{l_{\min}}-x_{l-1}-x_l),$$

subject to

$$\begin{aligned}
\Phi_i(\mathbf{Z})-(x_i+x_{i+1}) &= 0, && i=1 \ldots p_1,\\
\Phi_i(\mathbf{Z})-Q\,\frac{i-p_3-0{\cdot}5}{m-p_3} &, && i=p_3+1 \ldots m,\\
\Delta_k(\Phi) &\geqslant 0 && \text{for every } k,\\
x_{l+1}-x_l &\leqslant 0, && l=l_{\max} \ldots l_{\min},\\
0 \leqslant x_1 &\leqslant \tfrac{1}{3}, &&\\
x_i-x_{i+1} &\leqslant 0, && i=1 \ldots p_1,
\end{aligned} \tag{31}$$

where k is the index of a free element point on the shape, l is the index of the free nodal points on the shape and i is the index of the free nodal points on the surface.

If we give starting values for the free nodals on the shape and the free surface nodals, we can calculate the solution with the model (31). In every iteration step of (31) we have to solve Φ and Q with (24) and (22h).

7. FINAL REMARKS

In Section 4 we defined a model to solve the free surface and the discharge problem for the flow over a weir. The results in Section 5 are satisfactory. The extended optimization model to find the shape of a spillway is not tested, but it can be used as a starting point for further study.

REFERENCES

1. S. T. K. Chan, B. E. Larock and L. R. Hermann, 'Free-surface ideal fluid flows by finite elements', *J. Hydraul. Div., ASCE*, **99**, 959–975 (HY6), (1973).

2. K. Washizu and T. Nakayama, 'Applications of the finite element method to some free surface fluid problems', *Finite Elements in Water Resources*, Pentech, London, 1976.
3. H. Dierch, A. Schirmer and K. Busch, 'Analysis of flows with initially unknown discharge', *J. Hydraul. Div., ASCE*, **103**, (HY3), (1977).
4. M. J. O'Carroll and E. F. Toro, 'Numerical computations of critical flow over a weir', *Int. j. numer. methods fluids*, **4**, 499–511 (1984).
5. J. M. Aitchison, 'Numerical solution of a free surface problem by a boundary element method', *Int. j. numer. methods fluids*, **8**, 91–96 (1988).
6. V. T. Chow, *Open Channel Flow*, McGraw-Hill, 1959.
7. F. M. Henderson, *Open Channel Flow*, MacMillan, New York, 1966.
8. M. Ikegawa and K. Washizu, 'Finite element method applied to analysis of flow over a spillway crest', *Int. j. numer. methods eng.*, **6**, 179–189 (1973).
9. J. M. Aitchison, 'A finite element solution for critical flow over a weir', *Proc. 3rd Int. Conf. on Finite Elements in Flow Problems*, Banff, Alberta, 1980.
10. E. F. Toro 'Finite element computation of free surface problems', *Ph.D. Thesis*, Mathematics Department, Teeside Polytechnic, Middlesbrough, 1982.
11. E. Varoglu and W. D. L. Finn, 'An inverse variable domain finite element technique for irrotational flow problems with free surface', *Int. Symp. on Innovative Numerical Analysis in Applied Engineering Science, Session 4*, Versailles, 23–27 May 1977.
12. C. A. Brebbia, *The Boundary Element Method for Engineers*, Pentech, London, 1978.
13. C. A. Brebbia and S. Walker, *Boundary Element Techniques in Engineering*, Newnes–Butterworths, 1980.
14. C. A. Brebbia, *Progress in Boundary Element Methods, Vol. I*, Pentech, London, 1981.
15. J. N. Sneddon, *Elements of Partial Differential Equations*, McGraw-Hill, 1964.
16. M. A. Jaswon and G. T. Symm, *Integral Equation Methods in Potential Theory and Elastostatics*, Academic Press, London, 1977.
17. J. E. Romate, 'Een randintegraal method voor vrije oppervlakte problemen', Delft Hydraulics Laboratory, 1984.
18. K. Schittkowski, 'NLPQL: a Fortran subroutine solving constrained non-linear programming problems', *Ann. Oper. Res.*, **5**, 485–500 (1986).
19. H. T. Falvey, 'Air–water flow in hydraulic structures', U.S. Department of Interior, Denver, 1980.
20. E. J. Lesleighter and H. T. Chang, 'Experience on flow aeration to prevent cavitation erosion in spillway chute', *Conf. on Hydraulics in Civil Engineering*, Sydney, October 1981.
21. E. F. Toro and M. J. O'Carroll, 'A Kantorovich computational method for free surface gravity flows', *Int. j. numer. methods fluids*, **4**, (1984).